

# Fused Deposition Modeling and Fabrication of a Three-dimensional Model in Maxillofacial Reconstruction

Saman Naghieh<sup>a</sup>, Alireza Reihany<sup>b</sup>, Abbas Haghighat<sup>b</sup>, Ehsan Foroozmehr<sup>a\*</sup>, Mohsen Badrossamay<sup>a</sup>, Foroozan Forooghi<sup>a, c</sup>

<sup>a</sup> Department of Mechanical Engineering, Isfahan University of Technology, 84156-83111, Isfahan, Iran; <sup>b</sup> Department of Oral and Maxillofacial Surgery, Dental Implants Research Center, School of Dentistry, Isfahan University of Medical Sciences, 81746-73461, Isfahan, Iran; <sup>c</sup> Noura Imprinting Layers Industries, Isfahan Science and Technology Town, 84156-81999, Isfahan, Iran.

**\*Corresponding author:** Ehsan Foroozmehr, Department of Mechanical Engineering, Isfahan University of Technology, 84156-83111, Isfahan, Iran. **E-mail:** eforoozmehr@cc.iut.ac.ir; **Tel:** +98-31 3391 5238

**Submitted:** 2016-03-27; **Accepted:** 2016-05-12

The utilization of customized three-dimensional (3D) models based on patient's computed tomography (CT) scan data and by assistance of additive manufacturing/rapid prototyping (AM/RP) techniques for 3D reconstruction is one of the applicable trends for reducing the errors and time saving during surgeries. In the present study, the methodology of the fabrication of a custom-made 3D model based on converting CT scan data to standard triangle language (STL) format for a 33-years old male patient who was suffering from an accident trauma was described. The 3D model of the patient's skull was fabricated and applied in preoperative planning. It was used for designing a comprehensive plan for rehabilitation of the damaged orbit to restore the appearance and bone reconstruction of the patient. Before fabricating the model, the accuracy of protocols used in converting CT scan data into STL file was evaluated. Then, the model was fabricated by a fused deposition modeling (FDM) machine. Using this procedure led to a maximum of 1.4% difference between the virtual model in the software and the fabricated 3D model in the fracture site. The present technique reduced operation time significantly. In addition, following eight months from the operation, the treatment approach ensured the patient's fractures healing process.

**Keywords:** Computed tomography; Orbital cavity; Reconstruction; Three-dimensional printing

## Introduction

Additive manufacturing/rapid prototyping (AM/RP), a technology that has been applied vastly in different aspects of industry, provides design free form and environmental benefits. It is defined as the process of combining materials based on layered manufacturing to fabricate objects from 3-dimensional (3D) models (1,2). In recent years, combination of image processing and AM techniques has been utilized as an appropriate method for 3D reconstruction in medicine and especially in oral and maxillofacial surgery (3). Not only is maintaining anatomic uniformity and appearance one of the vital factors for reconstruction of defects in maxillofacial diseases; in addition, it restores ocular function (4). In the conventional approach, in oral and maxillofacial reconstruction, anthropological analyses of the facial skeleton has to be done with more invasive methods in order to reach the essential physical reconstruction of the entire bones. Consequently, significant contamination of the original bones could occur. Furthermore, it is widely accepted that shaping plates; for

instance, during the operation in the conventional method, depends mainly on the sculpting skills of the surgeon. As a result, it increases the hazard of a second interference; consequently, causes additional concern for the patients (5). The AM techniques have been reported to be capable of eliminating such drawbacks of the conventional maxillofacial surgical procedures (6). Also, it could reduce the operation time in the conventional method (7). 3D models, fabricated by AM techniques, are versatile appliances for diagnosis in congenital malformations, craniomaxillofacial defects, pathologies and reconstruction. Other applications are in maxillofacial trauma, orthognathic, facial asymmetry surgeries, surgical planning, and custom prosthesis design (8). Using pre-operative 3D model for a traumatic patient can improve surgical procedures and the outcomes without any intra-operative complications (9). Furthermore, it has become progressively more popular by orthopedic surgeons (10). For instance, it was reported in some cases, reconstruction in the wrong plane has been done because of limited surgical fields throughout the surgery of orbital wall fractures. This is precisely where benefiting from 3D model

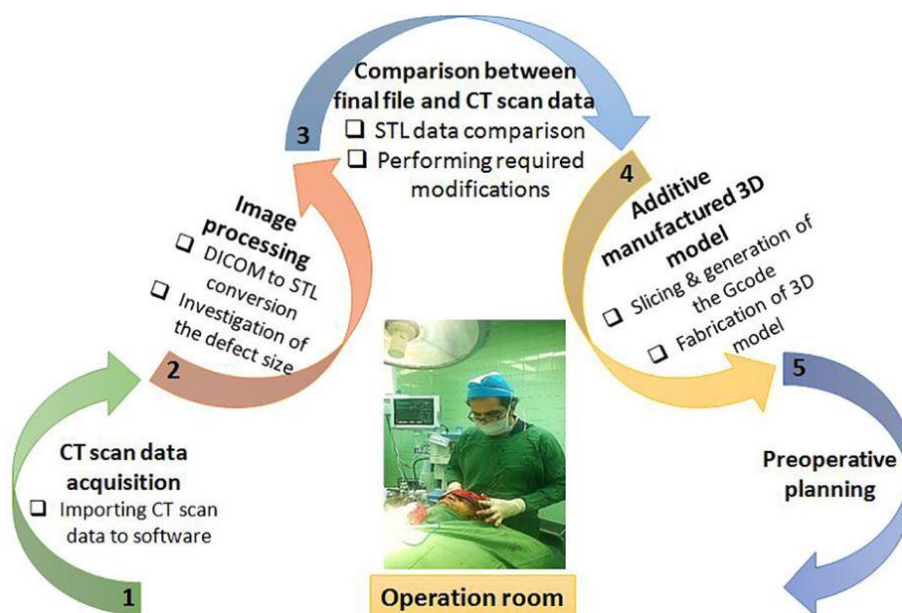


**Figure 1.** The procedure of converting CT scan data into the final 3D model

shows its role; nonetheless, this model prevents any malpositioning of implant material (11). In this regard, using bio-models for reaching predictable outcome was done as an appropriate method for orbital wall reconstruction by Tang and his co-workers (12). In addition, AM techniques can be used in the production of occlusal splints and maxillofacial prosthetics. It can also get applied in orthodontic treatment for the invisible orthodontic appliances (13). Moreover, intraoperative navigation can be accompanied with computer aided design (CAD) and 3D model for facial reconstruction (14).

There are different types of AM techniques and the oldest one, stereolithography, dates back to the late 1980s (15). It was first applied in maxillofacial surgery by Brix & Lambrecht in 1985 (16). Other techniques include selective laser sintering (SLS) (17), 3D printing (Binder-Jet) (18), fused deposition modeling (FDM) (19), direct metal laser sintering (DMLS) (20), laminated object manufacturing (LOM) (21), and electron beam melting (EBM) (22). However, The materials which are used in these techniques; such as, metal powder, ceramic powder, alloy metals, photopolymer, paper, foil, plastic film and titanium alloys could be thermoplastics (23).

Generally, FDM method is based on depositing of molten thermoplastic material onto a substrate layer by layer. FDM as a low-cost 3D printer and a profitable method is employed in various medical applications (24). As an outstanding example, it was used for fabricating the region of interest of the maxilla for the reconstruction of atrophic maxillary arches (25).

The present technical note explains the technique of fabrication of 3D model for pre-operative planning, as well as, investigation of the raw computed tomography (CT) scan data. It also describes possible errors in the process of converting raw data into standard triangle language (STL) file. The model is used in order to reconstruct the patient's damaged part and, especially, has a prepared plan for the orbital cavity before surgery. The aim of this project as a multi-disciplinary case involving engineers and anthropologists was fabrication of an economical custom-made 3D model with an acceptable accuracy.

## Technical note

In this study, a 33 years old male with occupational accident had multiple traumatic fractures in his facial bones. The patient suffered from lacerations on his face, facial contour deformity on the left side and diplopia on binocular vision. Based on CT scan images, the orbital rim and floor on the left had comminuted fractures; the zygomaticofrontal suture and zygomatic bone also were broke down on the left side of his face. The most challenging part of facial bones fracture was nasal bone fractures with a telescopic depressed fracture that could not get fixed by closed reduction. Thus, the facial soft tissue laceration was sutured in the emergency operation room, and the treatment of multiple fractures was decided to be performed later on, when the patient was stabilized neurosurgically.

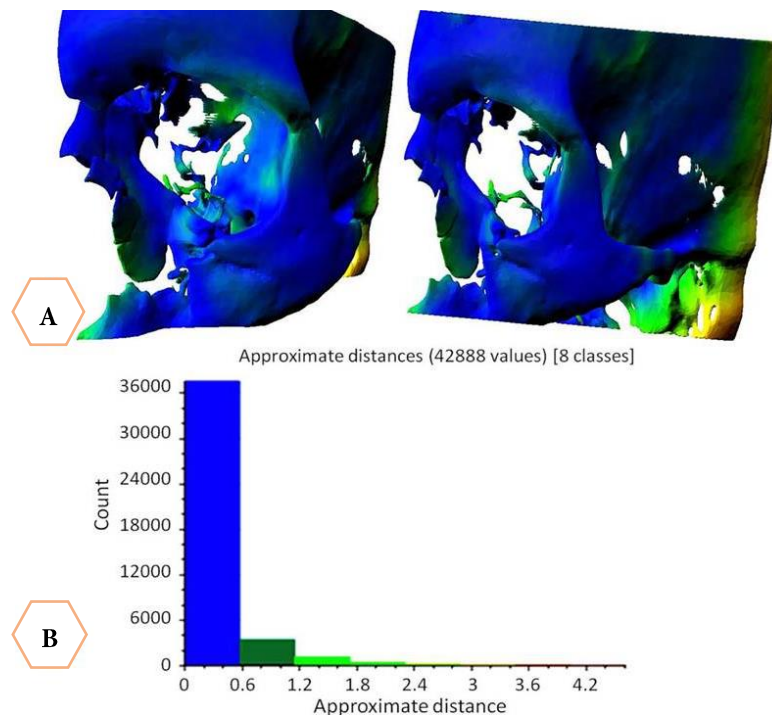


**Figure 2.** (A) Comparison between raw CT scan data and the final STL file: outcome of the CloudCompare® software; (B) and histogram of the intersection between final STL and CT scan data

## Preparation of the 3D model for preoperative planning

### Imaging and image processing

Figure 1 shows the procedure of converting CT scan data into the final 3D model used for the operation planning. As indicated, raw CT scan data was obtained from CT scan radiography. Images were acquired from the patient's head by using a General Electric Lightspeed VCT 64 Slice CT device® (General Electric, Michigan, United States) with slice increment of 0.625 mm at Alzahra Hospital (Isfahan, Iran). The peak voltage and the tube current were adjusted to 100 KVp and 210 mAs, respectively. Following generating STL format from the images by Mimics® 10.1 software (Materialise, Belgium) and verifying the accuracy and comparing these data to the raw CT scan data using CloudCompare® V2 (version 2.6.1) software. The outcomes of this comparison showed that there was an acceptable interface between final STL and the CT scan data (Figure 2A, B). The mean distance and standard deviation of calculations for this comparison were 0.223 and 0.437 mm, respectively. Moreover, critical regions (vicinity of the patient's orbit) had acceptable accuracy (blue regions) and were reliable for preoperative planning.

The STL file was imported in the slicing software for generating the required file format for the FDM machine. The 3D model was then fabricated to be used for the operation planning and during the operation.

## Fabrication of the 3D model

After making sure about the final STL file accuracy, its fabrication was performed. The slicing process was performed by using XYZware® software (version 1.1.34.8, XYZprinting). The model was then fabricated using XYZ printer. The material was ABS (white) which was supplied by XYZ printing. The process parameters of the machine were layer thickness 0.2 mm and temperature 260 °C. A manual post-processing of the prepared 3D model was performed in order to remove the support material

## Surgical procedure

Following inducing of general anesthesia, bicronal flap elevation for improving access to the orbital rim and nasal bone fractures without a visible scar, accompanied with subciliary, and maxillary vestibular incision. For depressed nasal septum defect, the cranial bone graft was anticipated and the orbital rim, as well as, the floor was reconstructed with plate and screw. In this step, there was a question whether to use a prosthetic sheet like Medpore for orbital floor or not. Hence, after the fabrication of the 3D model with acceptable accuracy, the process of preoperative planning was commenced by volume rendering. It is worth mentioning that the entire measurements were performed by a digital calliper.

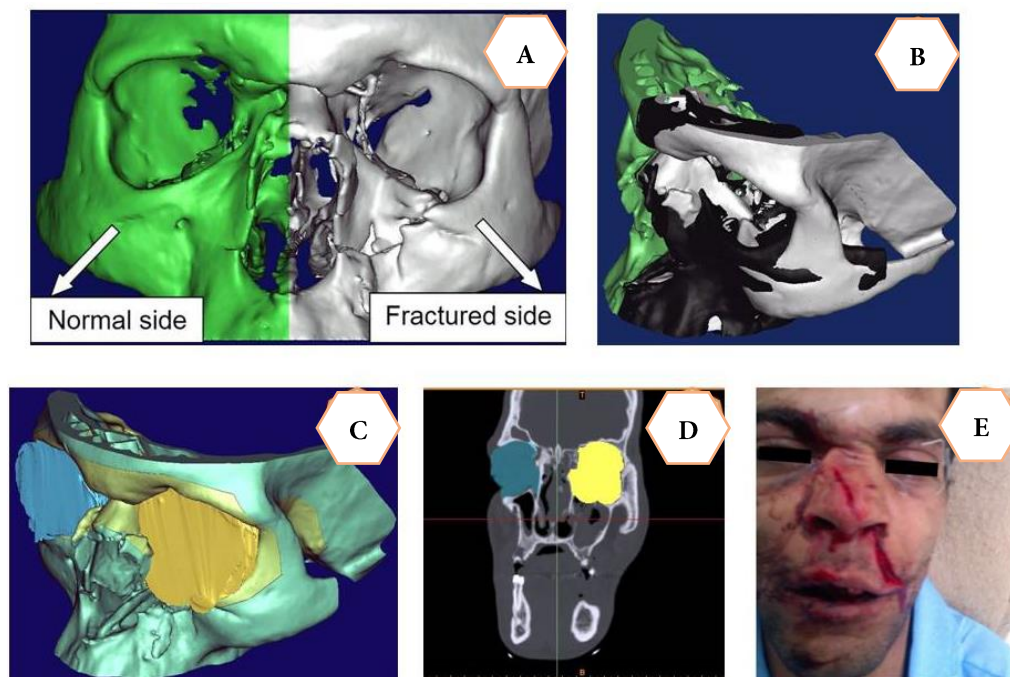


**Figure 3.** (A) The front view of the virtual 3D model of the patient; (B) asymmetrical patient's head (black part was generated by the mirroring technique); (C) volume rendering of 3D; (D) 2D object CT scan (fractured side has less than 10% more volume rather than normal side); (E) and front view of the patient before the surgery

Rose wax was also used to fill the fractured zones and form the final reconstructed orbital cavity. Moreover, for the reconstruction of nasal bone, spectrum photo polymer was placed in its proper location and formed. Then, it cured by Bredent PolyLux (20). The 3D model was sterilized and used in the operation room for more plate and prosthetic sheet formation and for bony distance measurements. Furthermore, for predicting the size of the graft harvest, which was essential for the nasal septum reconstruction, photopolymer resin was used in order to simulate the graft harvest that the surgery team had decided to cut from the cranial bone of the patient's head (Figure 4G).

It is quite essential to mention that mirroring the technique was not used for calculation of the amount of fractured site in the patient's head. There were numbers of large regions of the mirrored side deviating from the actually fractured side. Therefore, due to the asymmetrical form of the patient's head, mirroring technique was not a proper method to estimate the increase in the orbital cavity. As a substitution, multiple slicing was applied in Mimics® in order to virtually fill the orbital cavity with an appropriate amount of material. In addition, in order to increase the level of uniformity between both fractured and normal cavities, numbers of measurements were performed to determine the amount of plates and their form before surgery.

## Follow-up

The patient was monitored for eight months, and after this period; the status of the reconstructed zones was investigated using CT scan images. For a better understanding of the quality of the applied protocol, the data from last comparison between pre- and post-surgical CT scan was done based on determining the mean absolute difference of data (29). Therefore, firstly, the data from both groups were transferred to CloudCompare® and then moved in order to make the same coordinate system. After this step, CAD mesh inspection was performed. The results are shown in **Error! Reference source not found.H**. The results showed appropriate reconstruction near the fractured sites.

## Discussion

In the present patient, pre-fabricated 3D model was utilized and volume measurements was performed to account the volume differences between the right (normal side) and left (fractured side) orbital cavity. One of the main trends used for volume rendering is mirroring technique. It is used to generate the CAD model of the damaged bone based on another healthy site of the face (7). As an illustration, Saldarriaga *et al.*, utilized this technique in the manufacturing of customized implant for a patient with skull hole (28).

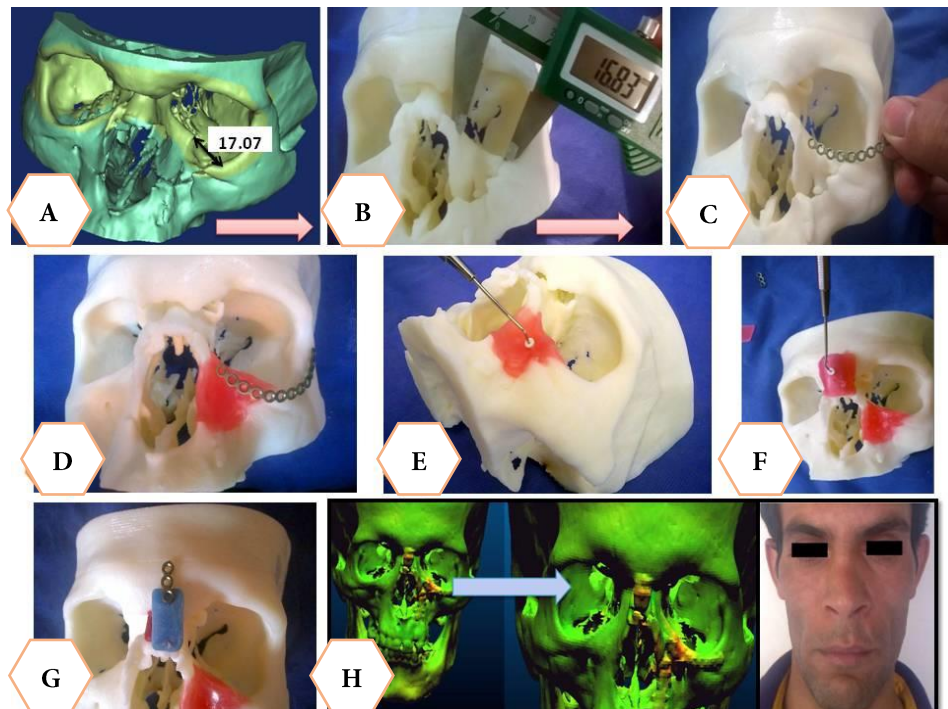


**Figure 4.** (A) Virtual measurement of the fractured side; (B) measurement of the distance between outer most surfaces of the formed plate; (C) the fractured bone and formed plate on the 3D model; (D) recreation of the damaged part with rose wax: front view; (E) side view; (F) reconstruction of the nasal septum via wax; (G) reconstruction of the nasal septum via photopolymer; (H) and comparison between pre- and post-surgery CT scan data as well as the front view of the patient after eight months

Figure 3A shows the fractured (white) and normal (green) sides of the skull. The normal side was mirrored to form the hypothetical shape of the fractured side, as shown in Figure 3B by black colour. Due to the asymmetrical problem, the volumetric calculation was done as indicated in Figure 3C. 2D object CT scan of the skull, as well as, the front view of the patient before the surgery, (Figures 3D and 3E).

After estimating the fractured volume in the orbital cavity, it was concluded that the increase in the orbital cavity volume is less than ten percent. Therefore, no prosthetic sheet was needed for orbital floor reconstruction.

Figure 4A indicates one of the measurements at the bottom of the orbital cavity that was used for cutting and forming the plate. After this step, the distance between the outer surface of the formed plate and the fractured bone was measured (Figure 4B). Then, data was compared by the software data analysis to ensure correct reduction and facial bone contour formation. The maximum difference between the virtual model in the software and real 3D fabricated model was about 1.4%. Figure 4C shows the last formed plate on the 3D model. The depth of the wax at different locations was compared with the model data. The results revealed a proper match between the digital data and the model (Figure 4D and E). Similar procedure was used for the nasal septum modification (Figure 4F).

## Conclusion

The pre-fabricated 3D model helped the surgeons to reduce the surgery time significantly and the results of the surgery demonstrated successful application of an accurate 3D printing method to be used in fabricating pre-operative models.

The proposed protocol could globally get recognized as a novel and simple protocol, in the field of maxillofacial surgery. Nonetheless, this protocol could be used worldwide because of using FDM technique, also because of checking the data accuracy before printing. As a matter of fact, by comparing the final data with initial data from CT scan in this new protocol, we could fabricate a unique 3D model with quite sufficient accuracy.

## Acknowledgement

The authors would like to appreciate Ahmad Foroozmehr from Noura Imprinting Layers Industries for his assistant in fabricating the 3D model.

Conflict of Interest: 'None declared'.



## References

1. Bikas H, Stavropoulos P, Chrysosolouris G. Additive manufacturing methods and modelling approaches: a critical review. *Int J Adv Manuf Technol* 2015;1-17.
2. Teeter MG, Kopacz AJ, Nikolov HN, Holdsworth DW. Metrology test object for dimensional verification in additive manufacturing of metals for biomedical applications. *Proc Inst Mech Eng Part H J Eng Med* 2015;229(1):20-27.
3. Farré-Guasch E, Wolff J, Helder MN, Schulten EAJM, Forouzanfar T, Klein-Nulend J. Application of Additive Manufacturing in Oral and Maxillofacial Surgery. *J Oral Maxillofac Surg* 2015;1-11.
4. Bhumiratana S, Vunjak-Novakovic G. Concise review: personalized human bone grafts for reconstructing head and face. *Stem Cells Transl Med* 2012;1(1):64-69.
5. Sherekar RM. An Image Processing Approach For Mandible Reconstruction & Fabrication By Using Selective Laser Sintering (SLS). *Int J Eng Appl Technol* 2015;(January):57-66.
6. Eggbeer D, Bibb R, Evans P, Ji L. Evaluation of direct and indirect additive manufacture of maxillofacial prostheses. *Proc Inst Mech Eng Part H J Eng Med* 2012;226(9):718-728.
7. El-Katatny I, Masood SH, Morsi YS. Error analysis of FDM fabricated medical replicas. *Rapid Prototyp J* 2010;16(1):36-43.
8. Moraes DE, Lauria A, Mayrink G, *et al.* Evaluation of the use of biomodels in sequelae of maxillofacial trauma. *Int J Odontostomatol* 2013;7(1):113-116.
9. Morrison DA, Guy DT, Day RE, Lee GYF. Simultaneous repair of two large cranial defects using rapid prototyping and custom computer-designed titanium plates: a case report. *Proc Inst Mech Eng Part H J Eng Med* 2011;225(11):1108-1112.
10. Van den Broeck J, Wirix-Speetjens R, Vander Sloten J. Preoperative analysis of the stability of fit of a patient-specific surgical guide. *Comput Methods Biomech Biomed Engin* 2015;18(1):38-47.
11. Beliakin SA, Khyshov VB, Khyshov MB, Klimova NA, Saifullina SN, Ėizenbraun O V. Reconstruction of posttraumatic skull and facial bones injuries with the use of perforated titanium plates and meshes. *Voen Med Zh* 2012;333(12):12-17.
12. Tang W, Guo L, Long J, *et al.* Individual design and rapid prototyping in reconstruction of orbital wall defects. *J Oral Maxillofac Surg* 2010;68(3):562-70.
13. Al Mortadi N, Eggbeer D, Lewis J, Williams RJ. Design and fabrication of a sleep apnea device using computer-aided design/additive manufacture technologies. *Proc Inst Mech Eng Part H J Eng Med* 2013;227(4):350-355.
14. Bell RB, Markiewicz MR. Computer-assisted planning, stereolithographic modeling, and intraoperative navigation for complex orbital reconstruction: a descriptive study in a preliminary cohort. *J Oral Maxillofac Surg* 2009;67(12):2559-70.
15. Hnatkova E, Kratky P, Dvorak Z. Production of anatomical models via rapid prototyping. *Int J CIRCUITS, Syst SIGNAL Process* 2014;8(C):479-486.
16. Sinn DP, Cillo JE, Miles BA. Stereolithography for craniofacial surgery. *J Craniofac Surg* 2006;17(5):869-875.
17. Liao H, Lee M, Tsai W, Wang H, Lu W. Osteogenesis of adipose-derived stem cells on polycaprolactone-  $\beta$  -tricalcium phosphate scaffold fabricated via selective laser sintering and surface coating with collagen type I. *J Tissue Eng Regen Med* 2013.
18. Shanjani Y, Croos D, Amritha JN, Pilliar RM, Kandel RA, Toyserkani E. Solid freeform fabrication and characterization of porous calcium polyphosphate structures for tissue engineering purposes. *J Biomed Mater Res Part B Appl Biomater* 2010;93(2):510-519.
19. Hsu S, Yen H, Tseng C, Cheng C, Tsai C. Evaluation of the growth of chondrocytes and osteoblasts seeded into precision scaffolds fabricated by fused deposition manufacturing. *J Biomed Mater Res Part B Appl Biomater* 2007;80(2):519-527.
20. Grünberger T, Domröse R. Direct Metal Laser Sintering. *Laser Tech J* 2015;12(1):45-48.
21. Liu S, Ye F, Liu L, Liu Q. Feasibility of preparing of silicon nitride ceramics components by aqueous tape casting in combination with laminated object manufacturing. *Mater Des* 2015;66:331-335.
22. Cormier D, Harrysson O, West H. Characterization of H13 steel produced via electron beam melting. *Rapid Prototyp J* 2004;10(1):35-41.
23. Choi JW, Kim N. Clinical Application of Three-Dimensional Printing Technology in Craniofacial Plastic Surgery. *Arch Plast Surg* 2015;42(3):267-277.
24. Smith EJ, Anstey JA, Venne G, Ellis RE. Using additive manufacturing in accuracy evaluation of reconstructions from computed tomography. *Proc Inst Mech Eng Part H J Eng Med* 2013;227(5):551-559.
25. Ciocca L, Fantini M, De Crescenzo F, Corinaldesi G, Scotti R. CAD-CAM prosthetically guided bone regeneration using preformed titanium mesh for the reconstruction of atrophic maxillary arches. *Comput Methods Biomech Biomed Engin* 2013;16(1):26-32.
26. Huottilainen E, Jaanimets R, Valášek J, *et al.* Inaccuracies in additive manufactured medical skull models caused by the DICOM to STL conversion process. *J Cranio-Maxillofac Surg* 2014;42(5):e259-e265.
27. Dong Y, Mou Z, Huang Z, Hu G, Dong Y, Xu Q. Three-dimensional reconstruction of subject-specific knee joint using computed tomography and magnetic resonance imaging image data fusions. *Proc Inst Mech Eng Part H J Eng Med* 2013;227(10):1083-1093.
28. Saldarriaga JFI, Vélez SC, Posada MDAC, Henao IEBB, Valencia MECAT. Design and Manufacturing of a Custom Skull Implant. *Am J Eng Appl Sci* 2011;4(1):169-174.
29. Shandiz MA, MacKenzie JR, Hunt S, Anglin C. Accuracy of an adjustable patient-specific guide for acetabular alignment in hip replacement surgery (Optihip). *Proc Inst Mech Eng Part H J Eng Med* 2014;228(9):876-889.

**Please cite this paper as:** Naghieh S, Reihany A, Haghighat A, Foroozmehr E, Badrossamay M, Foroozan Forooghi F. Fused Deposition Modeling and Fabrication of a Three-dimensional Model in Maxillofacial Reconstruction. *Regen Reconstr Restor*. 2016; 1(3): 139-144.

